

Exposing AI-generated Videos: A Benchmark Dataset and a Local-and-Global Temporal Defect Based Detection Method

Peisong He, Leyao Zhu, Jiaxing Li, Shiqi Wang, *Senior Member, IEEE*, Haoliang Li, *Member, IEEE*

Abstract—The generative model has made significant advancements in the creation of realistic videos, which causes security issues. However, this emerging risk has not been adequately addressed due to the absence of a benchmark dataset for AI-generated videos. In this paper, we first construct a video dataset using advanced diffusion-based video generation algorithms with various semantic contents. Besides, typical video lossy operations over network transmission are adopted to generate degraded samples. Then, by analyzing local and global temporal defects of current AI-generated videos, a novel detection framework by adaptively learning local motion information and global appearance variation is constructed to expose fake videos. Finally, experiments are conducted to evaluate the generalization and robustness of different spatial and temporal domain detection methods, where the results can serve as the baseline and demonstrate the research challenge for future studies.

Index Terms—Video forensics, AI-generated video, temporal defects, generalization, robustness.

I. INTRODUCTION

Recently, the explosive growth of artificial intelligence generated content (AIGC) has catalyzed revolutionary developments in several fields, such as social media and entertainment industry. Due to its impressive controllability and diversity [1], researchers are starting to pay more attention to diffusion model for the generation of images [2], [3] and videos [4]. Compared with static images, videos contain temporal dynamic information to present better visual experience. Video diffusion models [5] are progressively used on several video-related applications, including video generation, which has evolved from producing basic animated digital characters to generating photorealistic videos. Among these applications, text-to-video generation garners significant attention, which can automatically generate videos controlled by text prompts.

On the other hand, cybercriminals can use video generation technologies to produce more realistic fake videos and online platforms, such as social networks, simplify the broadcasting

and sharing of videos, posing severe negative impacts on public safety. Therefore, there is an urgent need to study corresponding countermeasures. In contrast to video editing software, text-to-video generation methods are capable of modeling both spatial and temporal long-range relationships. Consequently, existing video forensic datasets are insufficient to satisfy the demands for forensic analysis of AIGC videos created by text-to-video generators and there is a lack of forensics tools designed to identify AI-generated videos.

To address the issues above, we first construct an AI-generated video dataset, which considers several advanced AI video generation algorithms to create fake videos with various contents. Besides, a novel detection framework based on local and global temporal defects is proposed. Based on this dataset, cross-domain evaluation are considered to analyze generalization and robustness of different methods. The main contributions of this paper are summarized as follows:

- 1) We propose an AIGC video forensic dataset incorporating a variety of video diffusion generators and zero-shot text-to-video generators. Various text prompts are used to ensure the diversity of spatial and temporal contents of generated videos. Besides, typical video lossy operations are considered to create degraded samples to simulate network transmission process.
- 2) According to the analysis of temporal defects in generated videos, we proposed a novel detection framework by considering local motion information and global appearance variation. Besides, channel attention based feature fusion is designed to expose fake video by combining local and global temporal clues adaptively.
- 3) Extensive experiments are conducted to evaluate the generalization capability in cross-generator scenarios and the robustness against lossy operations, including video compression and transmission error. Experimental results can be used as the baseline for future work.

II. RELATED WORKS

A. Video Generation Algorithm

The diffusion model was originally proposed for image generation [6], which includes a forward diffusion process and a backward denoising process. Diffusion-based image generation models can be controlled by different types of information, such as text prompts. Since video data can be treated as a sequence of images, Ho et al. proposed the earliest diffusion-based video generation algorithm, video diffusion

This work is supported by National Key Research and Development Program for Young Scientists under Grant 2022YFB4501300. (Corresponding author: Dr. Haoliang Li.)

P. He and L. Zhu are with School of Cyber Science and Engineering, Sichuan University, Chengdu, China (e-mail: gokeyhps@scu.edu.cn, zhulyscu@gmail.com).

J. Li is with the Department of Electrical and Computer Engineering, Carnegie Mellon University, Pittsburgh, US (email: jiaxingli@andrew.cmu.edu).

S. Wang is with the Department of Computer Science, City University of Hong Kong, Kowloon, Hong Kong (e-mail: shiqiwang@cityu.edu.hk).

H. Li is with the Department of Electrical Engineering, City University of Hong Kong, Hong Kong (e-mail: haoliang.li@cityu.edu.hk).

model [5], by extending the 2D U-Net structure of the traditional image diffusion models to a 3D structure. It can capture the spatial and temporal features jointly from video data. Then, Zhou et al. [7] constructed the prior work, MagicVideo, to leverage latent diffusion model (LDM) for text-to-video generation in the latent space, which improves the generation efficiency. More recently, the researchers [8], [9] incorporated spatial-temporal convolution and attention into LDMs for text-to-video tasks. Khachatryan et al. [4] utilized the pre-trained stable diffusion model to conduct zero-shot video generation, which reduces computational costs.

B. AIGC Multimedia Forensics Dataset

As generative networks became capable of producing high-resolution realistic images, forensic analyzers began to pay attention to the detection of AI-generated images [10]–[12]. In [11] and [13], authors constructed large-scale AI-generated image datasets, including GAN-based and diffusion-based generators. However, unlike static images, video data contains temporal information, that provides dynamic visuals. Besides, videos are stored and broadcast using lossy compression techniques, which reduce temporal redundancy by the inter-frame coding process, such as motion compensation. Therefore, there is an urgent need in the field of video forensics to construct an AI-generated video dataset.

III. AI-GENERATED VIDEO DATASET

A. Data Collection

The natural videos were collected from the Microsoft Research Video Description Corpus (MSVD) dataset [14], where videos in the MSVD dataset were crawled from YouTube. The MSVD dataset was originally constructed to study video captioning techniques, and each video has a description. Therefore, these associated captions of videos can be utilized as text prompts for the generation of fake videos (negative samples) by video generators. Specifically, the dataset comprises 1000 natural samples paired with 1000 negative samples for each generator, where each negative sample consists of 24 frames. In this dataset, four advanced diffusion-based video generators are considered, which obtains 96k fake frames in total.

B. Feature Analysis

The distinct features of the proposed dataset are analyzed.

1) *Various Contents*: We first analyze the semantic diversity for text prompts, which are used to control the contents of generated videos. Similar to [15], the statistical analysis is conducted in aspects of spatial and temporal contents, respectively. As shown in Fig. 1, spatial major contents can be summarized into eight groups, such as people and buildings. For temporal content, generated videos have rich motion information, which differ from static images.

2) *Various Video Generators*: In this dataset, various generators based on video diffusion model [5] and a zero-shot text-to-video model are considered. Specifically, three most popular and publicly released video diffusion models are selected, including ali-vilab [8], [9], zeroscope [16], and potat1 [17].

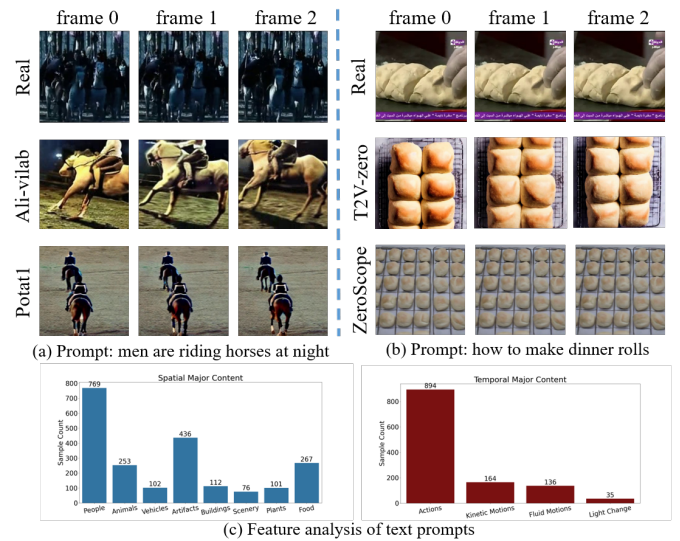


Fig. 1. Examples of AI-generated videos and feature analysis of our dataset.

Among them, ali-vilab is a text-to-video generation model using spatio-temporal blocks to conduct frame generation with temporal consistency and smooth motions. Following the similar generation pipeline, zeroscope and potat1 considers more fine-tuning strategies and other generation configurations, such as spatial resolutions. Besides, a zero-shot text-to-video generation method [4] is also considered, which utilizes the pre-trained image diffusion model and keeps temporal consistency with motion dynamics.

3) *Video Lossy Operations*: To simulate lossy operations during network transmission [18], [19], three kinds of video post-processing operations are considered to generate videos with quality degradation for robustness evaluation, including H.265 Average Bit Rate (ABR) compression, H.265 Constant Rate Factor (CRF) compression, and Bit Error. Each operation applies various degrees of operation intensity. Detailed settings are presented in Section V-D.

IV. DETECTION METHOD

AI-generated videos show different temporal dependencies compared with real videos, since their capturing and generation processes are dissimilar. Specifically, real videos are captured by camera devices, where the short time interval between adjacent frames leads to a very high temporal redundancy. On the other hand, AI video generators control the time continuity of frames in the latent space. These differences result in the defects of generated videos at different spatio-temporal scales. In this section, the proposed AI-generated video detection framework based on local and global temporal defects is presented in detail, as shown in Fig. 2.

A. Representation Learning of Local Motion Information

Due to the limitation of algorithm and computational cost, existing AI video generators are still hard to fully model the temporal characteristics of real videos. We tackle the problem

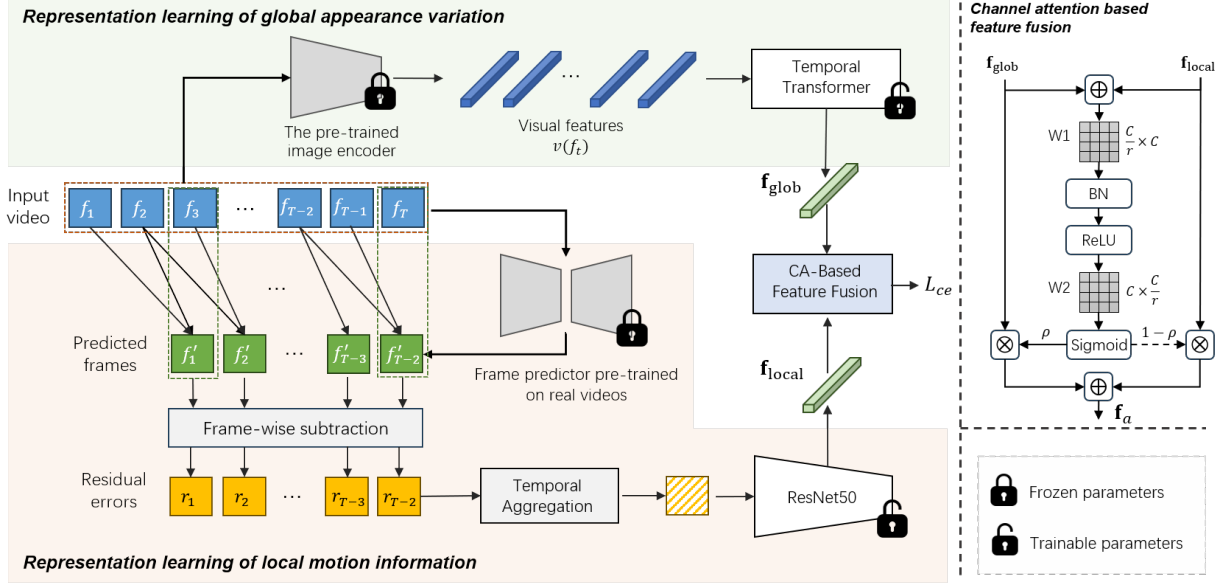


Fig. 2. The proposed AI-generated video detection framework based on local and global temporal defects.

of exposing abnormal motion patterns in AI-generated videos by measuring the predictability of inter-frame information.

1) *Extraction of Frame Prediction Error*: Inspired by the idea from anomaly detection [20], a frame predictor $P(\cdot, \cdot)$ is first trained by only using real videos to learn their “normal” motion patterns in local regions. Then, the parameters of this frame predictor are frozen. For an input video $\mathbf{F} = [f_1, f_2, \dots, f_T]$, two adjacent frames (f_t, f_{t+1}) are fed into $P(\cdot, \cdot)$ to obtain the predicted frame \hat{f}_{t+2} . Prediction errors can be calculated by $r_t = \hat{f}_t - f_t$ and the sequence of prediction errors \mathbf{R} is obtained ($\mathbf{R} = [r_1, r_2, \dots, r_{T-2}]$), which are used to measure the predictability of inter-frame local motion.

2) *Temporal Aggregation*: For real videos, the amplitude of their prediction errors is relatively small compared with fake videos due to high temporal redundancy. However, rich and diverse spatio-temporal contents may degrade the generalization capability of learned features. To address this issue, a temporal aggregation operator $A(\cdot)$ is designed for the sequence of prediction errors: $A(\mathbf{R}) = \hat{R}$ and $\hat{R}(i, j) = \frac{1}{T-2} \sum_{t=1}^{T-2} r_t(i, j)$. This simple and efficient strategy is applied to maintain long-range information and also mitigate the influence of various spatio-temporal details. Then, this aggregated prediction error map \hat{R} is fed into a 2D encoder ($F_l(\cdot)$), such as ResNet50, to obtain the local motion feature, $\mathbf{f}_{local} = F_l(\hat{R})$.

B. Representation Learning of Global Appearance Variation

Although AI video generators can model temporal continuity in the latent space, the lack of strong constraints for inter-frame consistency may cause abnormal variations of object appearances. For example, in the second row of subfigure 1(a), there is a distinct variation of person’s waist-to-leg proportions between “frame 0” and “frame 1”. We call this type of defects as abnormal global appearance variation.

To explore this clue, visual features of input frames are first extracted by a pre-trained image encoder, and then a transformer is applied to model their temporal variations. It should

be noted that we adopt the pre-trained image encoder on vision tasks instead of training it directly on fake frames, which aims to mitigate the overfitting issue to specific generation patterns. Specifically, BEiT v2 [21] is used as the pre-trained visual feature extractor in this work, which designs a masked image modeling framework. Its vector-quantized knowledge distillation can reduce the sensitivity of visual features to changes in image details and present high-level semantics.

Therefore, the representation learning process of global appearance variation can be expressed as follows.

$$\mathbf{f}_{glob} = F_t([v(f_1), \dots, v(f_T)]) \quad (1)$$

where $v(\cdot)$ denotes a pre-trained BEiTv2 model and $F_t(\cdot)$ is a trainable temporal transformer, where extracted visual features are used as input tokens with their temporal positions t .

C. Channel Attention Based Feature Fusion

In Section IV-A and IV-B, two types of representations are extracted to expose temporal defects caused by the AI video generation process. Due to the diversity of generator architectures and training strategies, AI-generated videos may exhibit various defects. To achieve more reliable detection capability, a channel attention (CA) based fusion module is designed to fuse \mathbf{f}_{local} and \mathbf{f}_{glob} , as shown in Fig. 2.

$$\rho_a = \delta(\text{BN}(W_2 \cdot (\text{ReLU}(\text{BN}(W_1 \cdot \mathbf{f}_t)))))) \quad (2)$$

$$\mathbf{f}_a = \rho_a \otimes \mathbf{f}_{local} + (\mathbf{1} - \rho_a) \otimes \mathbf{f}_{glob} \quad (3)$$

where $\mathbf{f}_t = \mathbf{f}_{local} \oplus \mathbf{f}_{glob}$. \oplus and \otimes denote the element-wise summation and Hadamard product, respectively. $W_1 \in \mathbb{R}^{\frac{C}{r} \times C}$ and $W_2 \in \mathbb{R}^{C \times \frac{C}{r}}$ denotes the parameters of fully-connected layers, which are used as channel context aggregators to exploit channel interactions. r is the channel reduction ratio.

$\text{BN}(\cdot)$ and $\text{ReLU}(\cdot)$ denote batch normalization layer and non-linear activation layer, respectively. $\delta(\cdot)$ denotes the Sigmoid function. $\mathbf{1}$ is the all-one vector. In this way, CA-based feature fusion module can adjust the significance of different channels to extract more generalized forensics clues. Then, the cross-entropy loss is considered to optimize the detection network.

V. EXPERIMENTS

In this section, we will evaluate the detection performance of spatial and temporal-based detection algorithms. For AI-generated video forensics in the open world, detectors need to be generalized for fake videos created by unseen generators. Besides, it is also significant to be robust against video lossy operations. Therefore, the generalization and robustness are evaluated in experiments.

A. Baseline Methods

Currently, there is a lack of detection algorithms designed for AI-generated videos. Therefore, we first select two advanced AI-generated image detection methods, including CNNSpot [11] and NPR [12]. CNNSpot is a typical detection method in the data-driven manner to expose spatial artifacts while NPR is the SOTA method that leverages neighboring pixel relationships to identify both GAN- and diffusion-generated images. Besides, video classification networks, including I3D [22], S3D [23], and their extended versions with residual connections (I3D_Res and S3D_Res) are also considered for comparison.

B. Experimental Settings

In experiments, videos are divided into three groups for training, validation, and testing with the ratio 8:1:1. Videos are decoded into frame sequences, where each video clip is constructed by including seven temporally adjacent frames. The pre-trained frame predictor in [24] is used to obtain \mathbf{f}_{local} . In the CA-based fusion module, r is set as 4. For all detectors, batch size is set as 64. The initial learning rate is set to 10^{-3} . Adam optimizer is used to update network parameters. The clip-level detection accuracy is used as the evaluation metric, where the threshold of prediction probability is set to 0.5. Please note officially released detectors in CNNSpot [11] and NPR [12] fail to detect our samples (accuracies are nearly 50% on average) and they are retrained on our proposed dataset.

C. Performance Evaluation on Cross-generator Scenarios

In this experiment, the generalization capability of detection methods for unseen video generators is evaluated. In the training phase, fake video clips obtained by a particular video generator are used to train detectors. Then, testing samples produced by all generators are used to evaluate performance. Experimental results are presented in Table I.

As shown in Table I, when training and testing samples are generated by the same generator, all methods can obtain a promising detection performance (about 98% on average). However, for cross-generator cases, spatial domain-based methods (CNNSpot and NPR) and traditional video

TABLE I
PERFORMANCE EVALUATION OF GENERALIZATION CAPABILITY CROSS DIFFERENT GENERATORS (%).

Train\Test		Ali-vilab	Potat1	ZScope	T2V-zero	Ave.
	CNNSpot	97.42	91.53	83.68	50.18	80.70
	NPR	97.48	85.17	79.78	49.81	78.06
Ali-vilab	I3D	96.55	77.53	59.85	62.21	74.03
	I3D_Res	97.90	93.86	72.31	72.98	84.26
	S3D	96.80	86.37	70.20	62.29	78.92
	S3D_Res	97.98	92.43	73.07	88.89	88.09
	Ours	99.41	94.03	77.36	93.02	90.96
	CNNSpot	77.60	98.45	87.42	65.18	82.16
	NPR	73.34	97.98	79.40	53.14	75.96
Potat1	I3D	70.04	93.44	84.52	71.39	79.85
	I3D_Res	73.74	95.46	75.59	61.62	76.60
	S3D	80.22	98.07	80.73	54.97	78.50
	S3D_Res	80.64	98.82	76.09	76.77	83.08
	Ours	94.45	99.33	90.24	82.16	91.55
	CNNSpot	67.09	90.54	98.15	52.26	77.01
	NPR	72.20	85.94	97.98	52.39	77.13
ZScope	I3D	60.70	82.25	95.38	49.76	72.02
	I3D_Res	78.38	92.18	97.40	52.45	80.10
	S3D	67.01	92.60	97.65	51.86	77.28
	S3D_Res	78.13	90.92	97.32	57.76	81.03
	Ours	94.71	98.92	97.74	87.97	94.83
	CNNSpot	50.00	50.02	50.04	100.00	62.52
	NPR	58.61	67.15	54.95	98.89	69.90
T2V-zero	I3D	50.00	51.01	50.34	100.00	62.84
	I3D_Res	50.00	50.00	50.00	100.00	62.50
	S3D	50.00	58.08	54.38	100.00	65.61
	S3D_Res	51.18	64.14	60.44	100.00	68.94
	Ours	86.88	95.29	88.56	99.33	92.52

classification networks suffer from distinct performance drops. In contrast, our proposed detection still achieves satisfactory accuracies in all cases, which demonstrates the efficiency of leveraging both local and global defects to expose AI-generated videos. It should be noted that the cross-generator scenario involving T2V-zero generator is the most challenging case. This result may be due to the fact that T2V-zero is developed based on the pre-trained image diffusion model and then calculates the temporal continuity, which exhibits severe domain shift compared with samples of other generators.

D. Robustness Evaluation Against Video Lossy Operations

In this experiment, the robustness against lossy operations is evaluated. Specifically, for the levels of severity $\{1, 2, 3\}$, Bit Error considers each of $\{10, 5, 3\} \times 10^5$ bytes with a bit error; H.265 ABR applies $\{50\%, 25\%, 12.5\%\}$ of the original bit rate; H.265 CRF sets quality factors as $\{27, 33, 39\}$. Samples from videos of normal quality (without conducting lossy operations) are used to train detectors, and degraded samples are used to assess their robustness.

As shown in Table II, all methods obtain their best results for raw data and suffer from a distinct performance degradation against lossy operations. In general, temporal detection methods have better robustness than spatial detection methods since temporal forensics clues, such as global defects, are more likely to survive under lossy operations. Besides, detection

TABLE II

ROBUSTNESS EVALUATION AGAINST DIFFERENT LOSSY OPERATIONS (%).

Lossy operations		CNNSpot	NPR	I3D_Res	S3D_Res	Ours
Raw Data	None	75.60	75.26	75.87	80.29	92.46
Bit Error	1	73.12	73.69	73.49	79.56	89.65
	2	71.80	72.20	71.94	78.81	90.31
	3	70.34	70.68	70.06	78.04	90.07
H.265 ABR	1	75.04	69.42	75.78	79.97	91.21
	2	74.72	67.99	75.46	79.52	89.45
	3	74.11	67.45	74.81	78.58	86.71
H.265 CRF	1	74.76	68.32	75.53	79.79	90.93
	2	74.18	67.44	74.80	78.87	88.24
	3	73.43	66.75	73.67	77.37	84.26

TABLE III

THE ABLATION STUDY OF KEY COMPONENTS (%).

f_{glob}	f_{local}	CA-based fusion	Acc
✓			88.56
✓	✓		89.52
✓	✓	✓	92.46

accuracies decrease with the increment of severity levels, where distortions caused by lossy operations become more severe on forensic clues. This result infers that it is necessary to develop robustness improvement strategies.

E. Ablation Study

In this section, key components of the proposed detection framework are evaluated incrementally, including f_{glob} , f_{local} and the channel attention-based feature fusion (CA-based feature fusion). f_{glob} is first evaluated independently and then combined with f_{local} using the simple feature concatenation. Finally, the CA-based fusion is applied to fuse f_{glob} and f_{local} .

As shown in Table III, only using f_{glob} can expose fake videos to some degree due to the limited generation ability of current video generators. When f_{local} is considered as the complement, detection performance is improved. Furthermore, the CA-based feature fusion can obtain a distinct performance gain by combining local and global temporal traces adaptively. This result infers that the properties of temporal defects in fake videos generated by different generators are various, which should be taken into consideration for obtaining more reliable detection results.

VI. CONCLUSION

To address the security issue of AI-generated videos, we constructed a benchmark video dataset, where samples are generated by several advanced diffusion-based video generators with various contents. Besides, typical video lossy operations are considered to create degraded samples. Then, a novel detection framework is proposed by jointly learning local motion information and global appearance variation, which captures defects at different spatio-temporal scales. To mimic the practical forensics scenarios, extensive experiments are conducted in aspects of generalization and robustness. This work can serve as a baseline for future work about video forensics in the upcoming AIGC era.

REFERENCES

- [1] C. Li, Z. Zhang, H. Wu, W. Sun, X. Min, X. Liu, G. Zhai, and W. Lin, "AGIQA-3K: An open database for AI-generated image quality assessment," *IEEE Trans. Circuits Syst. Video Technol.*, Early Access, 2023.
- [2] H. Chen, Y. Zhang, X. Wang, X. Duan, Y. Zhou, and W. Zhu, "DisenDreamer: Subject-driven text-to-image generation with sample-aware disentangled tuning," *IEEE Trans. Circuits Syst. Video Technol.*, Early Access, 2024.
- [3] X. Chen, J. Tan, T. Wang, K. Zhang, W. Luo, and X. Cao, "Towards real-world blind face restoration with generative diffusion prior," *IEEE Trans. Circuits Syst. Video Technol.*, Early Access, 2024.
- [4] L. Khachatryan, A. Movsisyan, V. Tadevosyan, R. Henschel, Z. Wang, S. Navasardyan, and H. Shi, "Text2video-zero: Text-to-image diffusion models are zero-shot video generators," in *Proc. IEEE Int. Conf. Comput. Vis.*, 2023, pp. 15 954–15 964.
- [5] J. Ho, T. Salimans, A. A. Gritsenko, W. Chan, M. Norouzi, and D. J. Fleet, "Video diffusion models," *Proc. Adv. Neural Inf. Process. Syst.*, vol. 35, pp. 8633–8646, 2022.
- [6] J. Ho, A. Jain, and P. Abbeel, "Denoising diffusion probabilistic models," *Proc. Adv. Neural Inf. Process. Syst.*, vol. 33, pp. 6840–6851, 2020.
- [7] D. Zhou, W. Wang, H. Yan, W. Lv, Y. Zhu, and J. Feng, "Magicvideo: Efficient video generation with latent diffusion models," *arXiv:2211.11018*, 2022.
- [8] Z. Luo, D. Chen, Y. Zhang, Y. Huang, L. Wang, Y. Shen, D. Zhao, J. Zhou, and T. Tan, "Videofusion: Decomposed diffusion models for high-quality video generation," *arXiv:2303.08320*, 2023.
- [9] Alivilab, "Ali-vilab, <https://huggingface.co/ali-vilab/text-to-video-ms-1.7b>," 2023.
- [10] B. Chen, X. Liu, Y. Zheng, G. Zhao, and Y.-Q. Shi, "A robust GAN-generated face detection method based on dual-color spaces and an improved Xception," *IEEE Trans. Circuits Syst. Video Technol.*, vol. 32, no. 6, pp. 3527–3538, 2022.
- [11] S. Wang, O. Wang, R. Zhang, A. Owens, and A. A. Efros, "CNN-generated images are surprisingly easy to spot... for now," in *Proc. IEEE/CVF Conf. Comput. Vis. Pattern Recognit.*, 2020, pp. 8692–8701.
- [12] C. Tan, H. Liu, Y. Zhao, S. Wei, G. Gu, P. Liu, and Y. Wei, "Rethinking the up-sampling operations in CNN-based generative network for generalizable deepfake detection," in *Proc. IEEE/CVF Conf. Comput. Vis. Pattern Recognit.*, Accepted, 2024.
- [13] M. Zhu, H. Chen, Q. Yan, X. Huang, G. Lin, W. Li, Z. Tu, H. Hu, J. Hu, and Y. Wang, "Genimage: A million-scale benchmark for detecting AI-generated image," *Proc. Adv. Neural Inf. Process. Syst.*, vol. 36, 2023.
- [14] D. L. Chen and W. B. Dolan, "Collecting highly parallel data for paraphrase evaluation," in *ACL-HLT - Proc. Annu. Meet. Assoc. Comput. Linguist.: Hum. Lang. Technol.*, 2011, pp. 190–200.
- [15] Y. Liu, L. Li, S. Ren, R. Gao, S. Li, S. Chen, X. Sun, and L. Hou, "Fetv: A benchmark for fine-grained evaluation of open-domain text-to-video generation," in *Proc. Adv. Neural Inf. Process. Syst.*, vol. 36, 2023, pp. 62 352–62 387.
- [16] S. Sterling, "zeroscope-v2, https://huggingface.co/cerspense/zeroscope_v2_576w," June. 2023.
- [17] Camenduru, "potat1, <https://huggingface.co/camenduru/potat1>," 2023.
- [18] J. W. Wells and A. Chatterjee, "Error-resilient video encoding using parallel independent signature processing," *IEEE Trans. Circuits Syst. Video Technol.*, vol. 27, no. 5, pp. 1077–1090, 2017.
- [19] Y. Li, X. Zhang, C. Cui, S. Wang, and S. Ma, "Fleet: Improving quality of experience for low-latency live video streaming," *IEEE Trans. Circuits Syst. Video Technol.*, vol. 33, no. 9, pp. 5242–5256, 2023.
- [20] R. Nayak, U. C. Pati, and S. K. Das, "A comprehensive review on deep learning-based methods for video anomaly detection," *Image and Vis. Comput.*, vol. 106, p. 104078, 2021.
- [21] Z. Peng, L. Dong, H. Bao, Q. Ye, and F. Wei, "BEiT v2: Masked image modeling with vector-quantized visual tokenizers," *arXiv:2208.06366*, 2022.
- [22] J. Carreira and A. Zisserman, "Quo vadis, action recognition? a new model and the kinetics dataset," in *Proc. IEEE/CVF Conf. Comput. Vis. Pattern Recognit.*, 2017, pp. 6299–6308.
- [23] S. Xie, C. Sun, J. Huang, Z. Tu, and K. Murphy, "Rethinking spatiotemporal feature learning: Speed-accuracy trade-offs in video classification," in *Proc. Eur. Conf. Comput. Vis.*, 2018, pp. 305–321.
- [24] X. Hu, Z. Huang, A. Huang, J. Xu, and S. Zhou, "A dynamic multi-scale voxel flow network for video prediction," in *Proc. IEEE/CVF Conf. Comput. Vis. Pattern Recognit.*, 2023, pp. 6121–6131.